Pulse-Induced Energy Gains in Electrochemical Systems

Experiment Findings *in* Journal of Electrical Electronics Engineering · August 2024

DOI: 10.33140/JEEE.03.04.05

1 author:

Julian Perry
Kerrow Energetics
11 PUBLICATIONS **0** CITATIONS

SEE PROFILE

ISSN: 2834-4928

Research Article

Journal of Electrical Electronics Engineering

Pulse-Induced Energy Gains in Electrochemical Systems

Julian Andrew Perry*

Kerrow Energetics, St Just, West Penwith, Cornwall, UK

***Corresponding Author**
Julian Andrew Perry, Kerrow Energetics, St Just, West Penwith, Cornwall, UK.

Submitted: 2024, Jun 24; **Accepted:** 2024, Aug 08; **Published:** 2024, Aug 12

Citation: Perry, J. A. (2024). Pulse-Induced Energy Gains in Electrochemical Systems. *J Electrical Electron Eng, 3*(4), 01-15.

Abstract

Inductively generated voltage transients, also known as flyback pulses or disruptive discharges, have traditionally been seen as a problem in analogue and digital electronics and a major component of electromagnetic interference (EMI). Despite this, originating in the 19th century and continuing to the present day, there have been continuous developments in the application of flyback pulses that are alleged to confer benefits to suitably engineered electrochemical and electromechanical systems. These benefits have spawned a long series of patents for such devices including pulsed and low-drag DC motors, efficient generators and battery chargers. However, despite the long history of such devices, there has been no clear and replicable scientific evidence provided to the peer community in support of the fundamental phenomenon of high voltage pulse induced energy gains, leading to misinformation and a range of misconceptions in both the amateur and professional domains.

In this first of two studies, a confirmatory research project has been transparently undertaken, using the Open Science Framework (OSF), and shown that inductive pulse charging (IPC) can result in energy gains and a Coefficient of Performance >1 in Lead-Acid and Lithium Iron Phosphate batteries when compared to controls using regular mains charging. Evidence has also shown a continuing effect on the electrochemistry after IPC has ceased and that the processes involved in the energy gains exhibit a distinct dynamic, and are not identical with, those in conventional charging. Some of the terms used by other researchers to describe these behaviours offer no descriptive value in the absence of a working theoretical model. For this reason, the usefulness of IPC as a low-powered energy source is unconfirmed.

Consideration is also given to how the most likely source of the measured energy gains can be determined, from either an internal electrochemical response to the voltage transients or from the local environment. These options carry with them implications for either transient induced enthalpic energy transfers in electrochemistry, or classical and quantum electrodynamic theory requiring the integration of the local environment and cross-boundary energy flows as part of a thermodynamically open system.

Keywords: Flyback Pulses, Inductive Pulse Charging, Pulsed DC, Coefficient of Performance, Open Thermodynamics

1. Introduction

Inductively generated voltage transients have traditionally been seen as undesirable electromagnetic interference (EMI) in analog and digital electronic systems and where they are either earthed or routed to less vulnerable pathways. However, claims that they can exhibit unusual properties, and can result in energy gains in secondary cells, have been made starting not long after the development of the first Lead-Acid battery in 1860 by Gaston Planté [1]. A significant number of scientists, engineers and experimenters, starting with Daniel Cook and Nikola Tesla in the late nineteenth century, Robert Adams, Edwin Grey, Raymond Kromrey and John Bedini in the twentieth, and others in recent times, made various discoveries that did not sit easily with the electrodynamic theory developed by Maxwell and substantially modified by Heaviside and Hertz [2-8]. Many electrical and mechanical engineers took the lead provided by Adams and Bedini in particular to build replications of DC pulsed motors and battery charging systems, even if they often did not always obtain the same performance and results. Adams (1993) designed a motor system that overcame one of the most persistent problems in electromechanical systems, that of the back EMF which served to increase drag and supply current as a function of rotor speed[1]. He also utilised the effect of the solenoid collapsing magnetic fields, producing what we now term 'flyback' or 'kickback' pulses, to further increase torque and provide an additional source of recycled energy for the system. His approach used one rotor to both trigger the production of pulses and provide a mechanical power output and a Coefficient of Performance (CoP) >1. He argued that the 'energy influx' his system demonstrated accessed energy from space itself on account of the 'far from equilibrium' conditions generated by the pulses and their interaction with the active vacuum which, since the development of Quantum Theory, was now considered a viable source of ambient energy under certain conditions [9].

Bedini, also drawing inspiration from previous researchers such as Tesla, Grey and such individuals as the renown 'non- linear' scientist Gabriel Kron, achieved a successful replication of the

patented Kromrey generator before going on to develop and demonstrate his own diverse range of generators. He also sought to replicate Kron's own achievement who, as chief scientist for General Electric on the U.S. Navy contract for the Network Analyser at Stanford University, reported on his development of several negative resistors that utilised an aspect of what has been termed the 'Heaviside energy component' [6,10].

Bedini continued to develop a wide variety of motors, generators, energisers and charging systems that similarly displayed a CoP>1 and his work has been explored and developed by many others and with many variants. In particular the work of Lindemann and Murakami have sought to provide access and detailed descriptions of how to replicate a basic device for others to use as a learning tool, thereby providing a groundswell of available technical information with which to examine and explore the key concepts and working principles [7]. They have shown how, with precise timing, a window of opportunity can be utilised to offset the effect of Lenz's Law on electromechanical systems and use it to support rotor momentum and the driving power supply.

In an attempt to bring together various energy harvesting technologies, Kelly assembled an unofficial compendium of technologies provided by divers researchers [11]. However, few were backed up with suitable scientific evidence, leaving the enquirer to make their own judgements and experimentation using the detailed information as a starting point. More recently, Striphan compared the performance of two types of circuit design, a conventional and a DC-DC boost converter, for use with a Bedini generator [12]. Inam developed a prototype of an 'Internet of Things' - based, 8 pole Neodymium magnet based prototype for a modified Bedini type generator and they proposed linking AI based tools to further enhance the potential of such generators [13]. Chrysocheris has shown that an alternative charging regime for Lithium batteries, using a pulse-charging algorithm instead of the conventional constant current-constant voltage method, can benefit charging efficiency and without a temperature rise [14]. The use of Bedini-type pulse generators was explored and advocated but with a need to find and use optimal settings for all the relevant parameters. Ali has showed how a purely magnetic motor can self-run with magnets in a so called Halback array, further supporting the move towards novel applications of magnetic fields, rotor and stator designs in non-standard arrangements [15]. Murad at Kepler Aerospace investigated the interdependence of dynamic force fields and how they are affected by space-time perturbations [16]. This suggests a connection with the use of voltage transients and 'far from equilibrium' events to disturb the local environment and which then results in various regauging processes and energy flows.

[1]*Robert Adams spent much of his career in broadcast engineering and served a term as the Chairman of the New Zealand section of the Institute of Electrical and Electronic Engineers, US*

[2]*A summary of the electrical and magnetic forces involved in a rotor based motor is presented in 'Engineering with Lenz's Law' at osf.io/kvnym*

Various theoretical models for the observed behaviours and energy gains of pulse systems exist and have been derived mainly from extrapolating mainstream theories and examining the various boundary conditions, limitations and assumptions of each. In some cases, there may be a need to re-evaluate a well established theory within a new context or set of operating conditions, requiring a reassessment of the reach and limitations of an accepted model. In particular the Maxwell-Heaviside electrodynamic model draws attention and enquiry as to whether its operating parameters are well fitted to non-linear or far-from-equilibrium conditions and various revision ideas have been proposed, especially due to the path of its historical reformulation under Heaviside and the other Maxwellians. For example, Eckardt shows how the development of ECE (Einstein-Cartan-Evans) theory which, like Relativity is a purely geometrical form, allows for spacetime itself to act as a source of energy and that, while gravitation is described by the curvature of spacetime, electromagnetism is represented by its spinning and the concept of torsion [17-19].

Links to the 2nd law of Thermodynamics, which is an axiom and not a theorem, may also be drawn and where over the past three decades there have been many experimentally supported challenges, not to the core principle, but to some aspects and embodiments of this 'supreme law of nature' [20]. Similarly, what are referred to as Type-B energetic process, conform to the 1st law of Thermodynamics but not all aspects of the second, unlike the more common Type-A that conform to both [21]. This has been evidenced in ATP synthesis in cells, for example, where highly asymmetrical boundary conditions apply that utilise ambient thermal energy for cell functions. It is not so far removed from this to propose that ambient electromagnetic energy may be utilised in situations where a high degree of asymmetry exists, induced by suitable non-linear and non-equilibrium events, such as those from high voltage transients. Many of the experimental findings over the last 120 years have resulted in the approval of a wide range of patents and which form the basis of various pulsed DC technologies[3]. While such experimentation has also been undertaken by keen amateur engineers and electricians as well as professionals, relatively little evidence has been formally submitted to the mainstream scientific community for peer review and examination, especially with regard to the direct effects of high voltage transients on secondary cells. As such, over the years, a considerable amount of misinformation, confusion and a number of misconceptions have arisen.

This first of two planned studies sets out to provide clear, confirmatory and replicable evidence of a phenomenon, an effect, namely that the flyback pulses used in inductive pulse charging (IPC) can result in energy gains in secondary cells and with a Coefficient of Performance (CoP) >1 when compared to regular mains charging. The study is based on six years of development and exploratory work, using various builds to explore a wide variety of operational parameters. In this way the optimum test conditions were developed to evaluate the main hypothesis and gain a better picture of the dynamics and effects of IPC on Pb-Acid and $LiFePO_4$ cells in particular. It is only when the phenomenon has been replicated by independent parties that a working theory can be developed, or suitable adaptations and revisions made to current electrodynamic theory

and with linkage to relevant aspects of thermodynamics and quantum theory.

Using the transparent OSF research framework, all the methodologies used, the data gathered and its analysis are publicly viewable in the project files, along with comprehensive replication information[4]. A second study will consider the most likely source of the energy gains, arising from either the battery's own electrochemistry or the local environment as an open system, together with some of the alleged benefits to battery State of Health (SoH), in particular the removal of hard sulphation and the restoration of charge capacity in Pb-Acid batteries. Once the likely source is confirmed then it is appropriate to explore more deeply the energetic processes and mechanisms that may be involved, as well as the scientific implications and the potential for energy harvesting.

[3]An article pre-print detailing the history of these technologies and speculative theories is at osf.io/w4m7r and a partial list of patents from the 1880's onwards is at: kerrowenergetics.org.uk/patents

[4]The OSF pre-registered project design is at osf.io/esr9h, and the files, research and replication data are at osf.io/ztfub/

2. Pulse Generator Design

The complete IPC system comprises two components, one generating the flyback pulses and the other, a battery, receiving them. The former behaves in full accordance with standard electrical theory with all the expected I^2R losses in the circuit and the magnetic hysteresis loses associated with the coils. The pulse generating component displays an internal efficiency $\boldsymbol{\eta}$ that can be measured using a large capacitor (55mF was used) as an energy receiver. The ratio of the energy input to that calculated as stored in the capacitor gave values of between 21% and 47%, depending upon the pulse repetition frequency (PRF) used and a value of 34% is applied to energy influx estimates described later.

It is only when the high voltage electrostatic pulses interact with the second component, the battery, at the positive cathode electrode, that energy gains and a CoP>1 are observed. Since the entire system operates with DC, there are no phase angles or reactive power factors to consider and which might otherwise be assumed to explain measured versus actual energy gains.

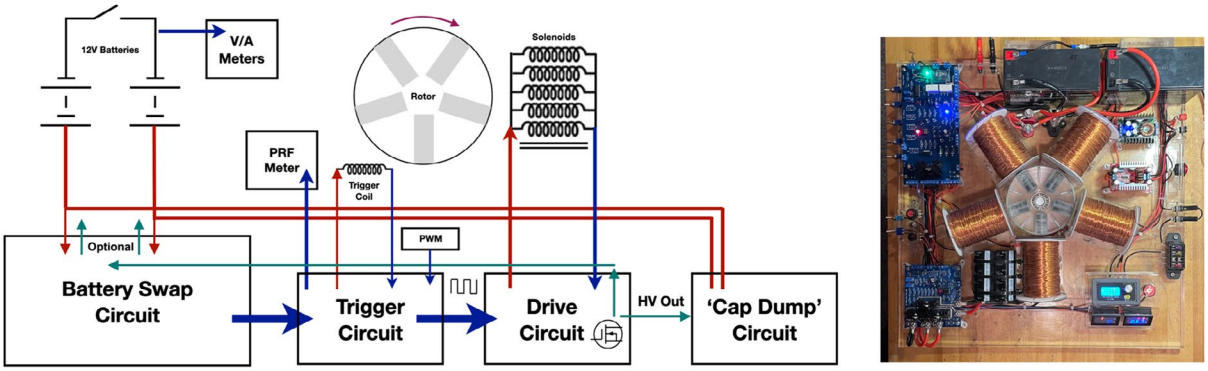

Figure 1: Generator system block diagram and build

Figure 1 shows a block diagram for the system, along with the build which allowed for many parameters to be investigated, including the use of high intensity capacitive discharges, so that for the study the most effective options could be employed. While the system can operate as a pulsed DC motor, using a rotor and multi-winding (litzed) coils to trigger and produce flyback pulses, for the study it was decided to use only the solid-state option. One reason for this was the ability to set the pulse repetition frequency (PRF) precisely to suit the battery being charged, in contrast to that resulting from using the rotor as the pulse trigger and which was rpm dependent and rarely optimised for a specific battery.

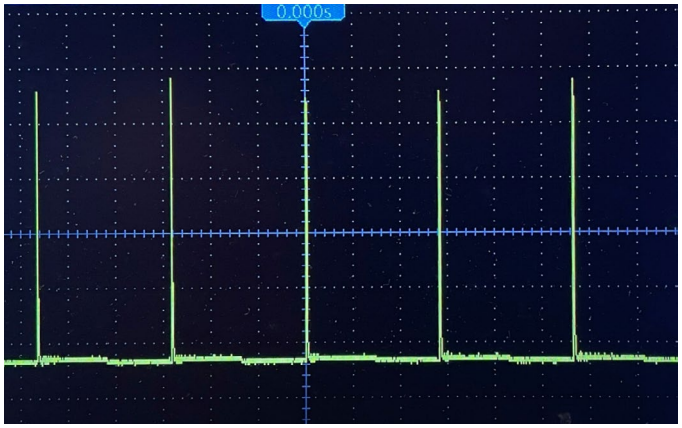

Figure 2: Fast 10µs rise and fall flyback pulse train

For the study, just three single winding coils were used and made from 2,500 turns of 0.71mm diameter enamelled wire and with an inductance of 320mH and a resistance of 14Ω. Connected in parallel they presented a combined inductance of 105mH at 4.6Ω and were switched with a purely solid-state mechanism using a single high-avalanche rated N-Channel power MOSFET and a pulse width modulation (PWM) unit for the trigger. The peak flyback voltage was limited by the avalanche rating of the active device (STW12N170k5), otherwise known as the 'Drain-Source breakdown voltage', rather than the coils themselves, which in this case was 1.7kV with a rise time of 10µs providing a dV/dt of 1.7 x 10^8 V/s.

Figure 2 shows a typical pulse train measured with a 10:1 potential divider. Preliminary work showed that using even higher voltages, such as with an insulated-gate bipolar transistor (IGBT) device, did not result in improved performance but tended towards generating more surface charge on the battery electrodes and which was not all converted to useful energy.

	Variable	Comments
1	Pulse repetition Frequency (PRF)	Set on PWM unit
2	%Duty	Set on PWM unit
3	Pulse kV	Limited by the active device used
4	%Ah charging point	% of nominal capacity, e.g. 90%
5	Charging time	Duration of pulse charging
6	Coil Load Voltage	Voltage across coils when operating
7	Coil Configuration	Including number of coils; affects the MMF
8	Discharge time	Affects IPC indirectly due to the 'after-effect'

Table 1: Key operating parameters for IPC

3. Parameter Setting

In order to operate the pulse system at peak performance, there are a range of adjustable parameters that need to be optimised. **Table 1** shows these variables, placed in the order with which they are ideally found and adjusted. Despite the sequence shown in this list, each variable does not function in isolation and has to be established using some temporary settings for all the other variables during each test. Since only one variable can be changed at a time, to ensure that any effects are due to this factor alone, this presents a dilemma since the CoP value is affected by all of them. For example, the PRF is not essentially more important than the charging time. Instead, there is a much wider range of values it can take and so it easier to start by setting this value first, even though it may take 30-40 test runs to do so. Once the PRF is optimally set then the other variables, with much narrower ranges, can be established much more quickly.

To overcome this issue, all the variables except the one you are testing for, can be set at a value most likely to give a reasonable performance and, to a large extent, this has been arrived at by experience and prior testing. For this reason, initial values are proposed for all the variables in **Table 2** and then, as each value is refined and confirmed, the measured performance increases towards its optimum.

Looking specifically at setting the PRF, all the batteries so far worked with have possessed an optimal PRF between the values of 50 - 200Hz. While it is unconfirmed, the internal plate design seems to have a considerable impact upon the optimum value. Pb-Acid batteries tend towards a design made up of a few large area plates of varying thickness depending upon the application, whereas Lithium batteries are made up of a large number of small cells, joined in series to give the required voltage and then as sets in parallel to provide the required capacity. Very loosely it appears that the smaller components of the Lithium respond to higher frequencies whereas the larger and thicker Pb-Acid battery plates respond to the lower end of the range. As can be seen from the values used in the OSF study, the optimum PRF for the 80Ah AGM Pb-Acid battery was 50Hz whereas for the 18Ah $LiFePO_4$ battery it was 155Hz[5]. Based on prior observations, for a small 7Ah $LiFePO_4$ battery, the optimum PRF is expected to be in the 100 - 200Hz range rather than the 50 - 100Hz range found for larger Pb-Acid batteries. Using the suggested values for all the other settings, as per **Table 2,** the procedure for establishing the PRF for a Lithium battery is to start at 100Hz and increment in step of 5Hz until a noticeable improvement is seen in the derived CoP value, even if it is a low value and < 1. The calculations and record keeping are facilitated by using the 'Data Processing Templates' and the 'Spreadsheet Guidance Notes' in the OSF Measurement files[6].

Test Type	Batt Ah	Start %Ah1	Trig.	Coils 2	Coil Load V	kV	Duty %	IPC t (m)	Rest t (m)	Disch. t (m)	Disch. I (A)
Lithium Solid State	18	~80	PWM	3P	11.75	1.7	22	8	0.1	4	4
Pb-Acid Solid State	80	~85	PWM	3P	11.75	1.7	18	50	0.1	5	4
1 % of nominal capacity at start of charging 2 Three coils connected in parallel 3 Between end of charging and discharge											

Table 2: Key operating parameters for IPC

Once an indication appears that you are approaching the optimum frequency then one can refine the settings with 1Hz increments. For example, if an improvement is noted for a 20Ah $LiFePO_4$ battery at 160Hz then one can test at 157, 158, 159 etc to 163Hz. Bear in mind that the performance falls off sharply either side of the optimum value so 1Hz makes a noticeable difference. This 'sharp' response is not seen as a form of actual resonance but rather the balancing of a set of competing factors. However, as and when a working theory for IPC has been developed then that understanding may change.

Once you have the best PRF to operate the PWM trigger and deliver pulses to the battery, then one can move on to adjust the other variables in sequence starting with the %Duty. Adjusting this value has a substantial effect on the current supply to the coils and this is the easiest and most flexible means of 'current limiting' by which the user supplied input current is controlled and minimised, resulting in a lower observable charging rate, but which can still result in a consistent energy influx due to the other factors that affect it and therefore a higher CoP.

Starting from the relevant value in **Table 2,** adjust downwards in 1% increments until you find a rapid fall off in performance, or the charging dV is insufficient to enable the 'discharge correction factor' to be calculated, as explained in the next section. If that occurs then various of the automated calculations in the spreadsheet cells will become invalid due to divisions by zero. It is also worth exploring incrementing upwards by the same amount to observe the effect on the charging graph and the resulting CoP. The other variables in the list can then be evaluated7 in a similar fashion and the overall performance will improve as each parameter is optimised.

[5]The optimum PRF for a larger 40Ah $LiFePO_4$ battery has recently been found to be 172Hz and where its construction is similar to the smaller 18Ah one but with a different number and set arrangement of the same type of small cells.

[6]These can be found at: https://osf.io/7mc8s/

[7]A fuller description of this process and for all the variables can be found in the 'Assembly & Guidance' manual in the Replication component of the OSF files at: osf.io/54qcn/

4. CoP Measurement Principle

By way of a summary of the principle used in the three measurement protocols, while we can know the electrical input energy to the device supplied by the user, we cannot directly know the total energy received by the battery. This is because of the unknown proportions of energy coming directly from the flyback pulses, by recognised mechanisms, and that coming from unknown sources. However, we can accurately determine the energy that can be discharged by the battery after pulse charging to return it to its starting voltage after a recovery and stabilisation stage. Due to its currently unknown origin, the energy gain in the system is simply referred to as the energy influx, or just the influx.

The basis of measuring the CoP then, in both the control and IPC tests, involves three distinct stages and one correction factor. The first is to charge the battery for a specified time from a measured starting voltage, using the relevant apparatus and monitored by a computerised battery analyser (CBA). This is followed by immediately discharging the battery to release a measurable amount of energy through an electronic load, also provided by the CBA.

The third stage is to allow the battery to rest for 60 mins during which its voltage recovers and stabilises and is then recorded as the final value. In the usual event that, due to the unknown amount of energy available for extraction, the final voltage after discharge was a little above or below the test starting value, then a correction factor was used to correct the discharge energy for what it would have been if the battery had been returned precisely to its original voltage and state of charge8. This factor is derived from the incremental charging and discharge voltages and, over the very small values of dV, is assumed to be linear.

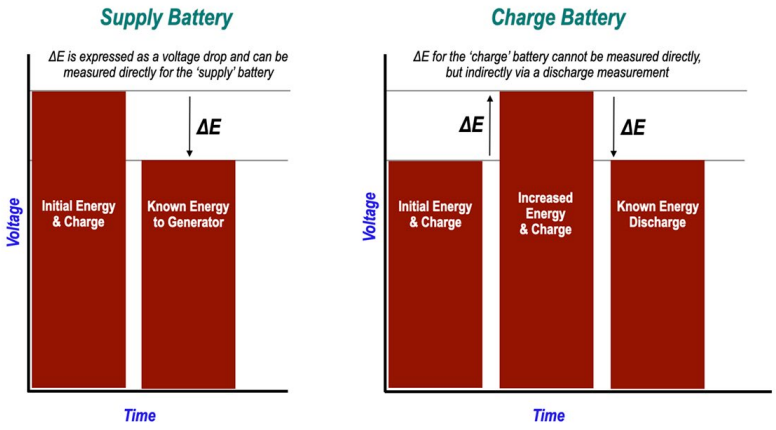

Figure 3: The main principle for CoP measurements

Figure 3 illustrates this process and, when the overall uncertainty has been derived from the various component uncertainties in the three stages (input, discharge and recovery) and the discharge correction factor, then a final CoP and uncertainty range can be given. The CoP value, as the ratio of the total energy output to the operator supplied input, is calculated from the measured input and output energies and not from the battery voltage increments which, particularly in the case of IPC, which

uses small supply currents, can be between 0.01 - 0.1V with the charging times used. For both the Control and IPC tests, an example will be given of the graphical data recorded (**Figs. 4** and **6)** in each stage of the process for the Pb-Acid and $LiFePO_4$ batteries respectively, along with a summary of the energy input and output and the derived CoP.

[8]*Battery voltage is an indirect measure of its energy content as expressed by the Nernst equation that relates the non-volumetric thermodynamically available energy (Gibbs energy) to the standard cell voltage.*

The experimental work was divided into three main stages: control experiments using appropriate mains chargers for the 80Ah AGM Pb-Acid and the 18Ah $LiFePO_4$ batteries, IPC experiments using the solid-state generator with batteries of identical capacity and type, and then 'closed-loop' (self-running) tests using a matched pair of the 18Ah Lithium batteries. Battery temperature was managed with a thermostatically controlled heating mat to maintain a temperature range of 18°C - 22°C to ensure that any temperature coefficients had minimal effect on the results. Each type of test was accompanied by a detailed methodology that provides the rationale, the practical stages and a fully worked example of how the CoP was derived in each case along with its uncertainty range. These methodologies and the process of uncertainty derivation are in the 'Protocols' component of the OSF project files at https://osf.io/ygqa3/ and a summary of all the data files for the measurements and analysis is provided at https://osf.io/y5ev3.

5. Control Tests

The main stages of a control test are the same as for an IPC test, the only difference being the charging equipment used. The battery charging and discharge cycles are conducted from a capacity of 90% of the nominal value. Charging was undertaken using a commercially available microprocessor controlled mains charger set to AGM mode. The input power was read directly after precisely 5 min charging using a wall socket power meter measuring in kWh, where 1kWh = 3,600kJ. The three stages of a control CoP test on the 80Ah AGM Pb-Acid battery are presented in **Figure 4.** Under the heading 'Parameters' is a summary of the variables used, readings, the various calculations and the derived uncertainty range. The resulting CoP data, for both the Pb-Acid and the $LiFePO_4$, batteries, was processed using the open source statistical package 'R' and a graphical plot produced and where each measurement uncertainty range is shown as an error bar. The control data plots are shown in **Figure 5.**

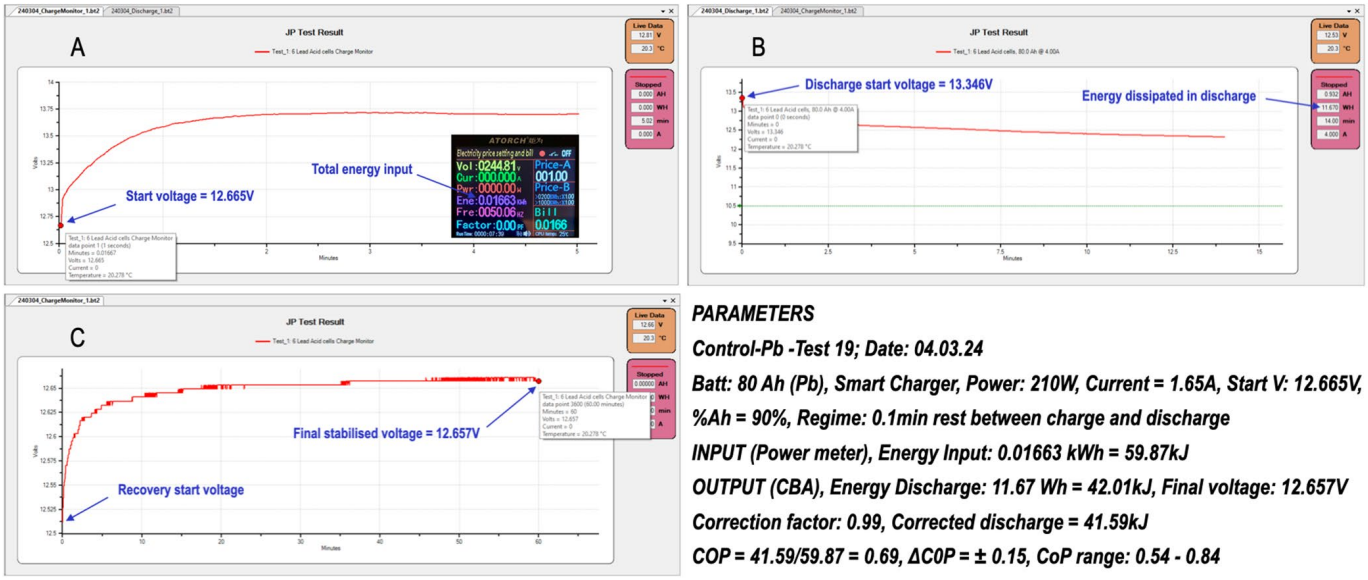

Figure 4: Combined graphs of the three stages of a control measurement test run with a) charging plot and energy input measurement b) discharge plot and energy dissipated c) recovery and stabilisation plot, and the summarised data with CoP calculation (full sized graphs are available in the 'Measurements' component of the project at: https://osf.io/frvzk/)

showed that regular mains charging of both battery types results in a CoP<1 with values of 0.69 ± 0.15 for the Pb-Acid and 0.79 ± 0.17 for the $LiFePO_4$. On the basis of the whole system presumed to behave in a closed manner, this equates to the standard efficiency η. Of note is the more efficient charging of the Lithium batteries compared to the Pb-Acid.

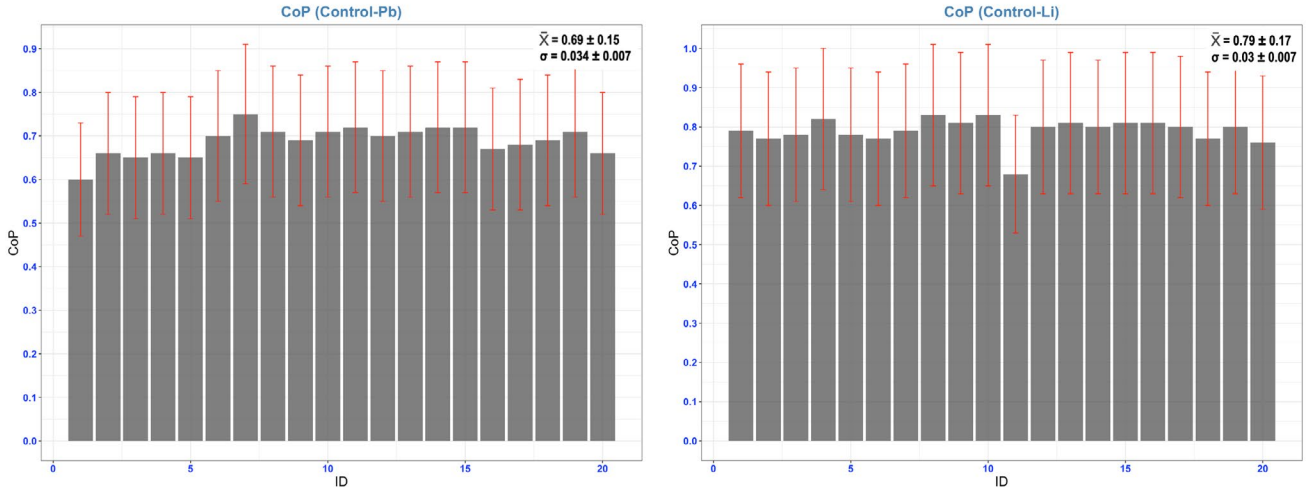

Figure 5: CoP values from control tests on Pb-Acid and $LiFePO_4$ batteries

6. IPC Tests

The methodology for measuring the Coefficient of Performance with IPC is the same as for the control tests except that the battery charging is undertaken with the HV pulse output from the flyback generator. As such, the input energy is calculated from the supply variables of voltage and average current from the power supply and the pulse charging time.

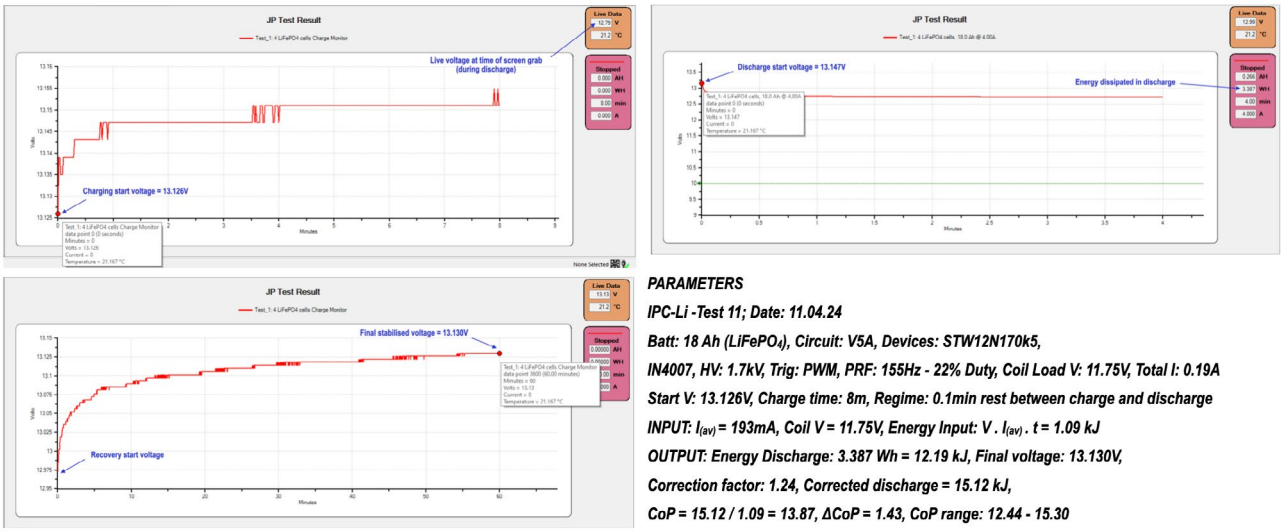

Figure 6: Combined graphs of the three stages of an IPC measurement test run with a) charging plot and energy input measurement b) discharge plot and energy dissipated c) recovery and stabilisation plot, and the summarised data with CoP calculation (full sized graphs are available in the '*Measurements*' component of the project at: https://osf.io/3b5dy/)

The parameters laid out in **Table 2** were used along with PRF values of 50Hz for the 80Ah AGM Pb-Acid battery and 155Hz for the 18Ah $LiFePO_4$ battery.

Figure 6 presents an example of graphs from the three stages of the measurement process and with the specific parameters and CoP derivation summarised on the right. As shown in the plots in **Figure 7,** the average Pb-Acid result was a CoP of 1.78 ± 0.21 and is typical of such measurements where larger capacity AGM format batteries are used. Here the use of thicker plates, to keep the internal resistance low, may serve to present a larger 'interaction cross-section'. In contrast, for the $LiFePO_4$ 18Ah battery, the average was 8.87 ± 3.36, therefore a range of 5.51 - 12.23 and with a peak value of 13.87 ± 1.43, indicating a much higher response to the pulses from, or via, the Lithium chemistry.

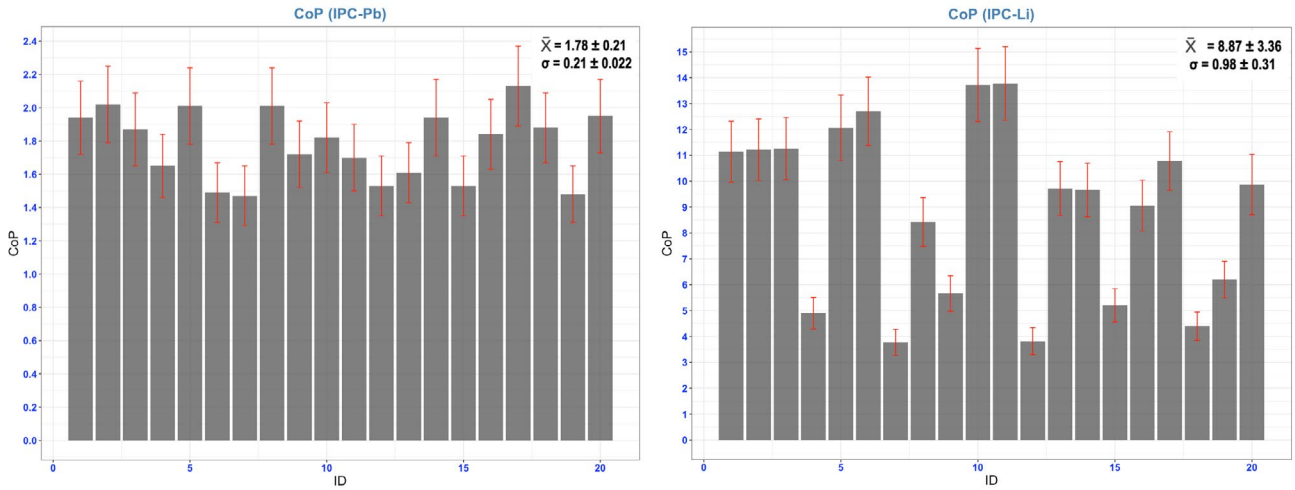

Figure 7: CoP values from IPC tests on Pb-Acid and $LiFePO_4$ batteries

These results may suggest that the even lower internal resistance of Lithium batteries may play an important role in their performance and also that the smaller atomic mass of Li^+ ions, with their higher Gibbs energy values[9], are able to react to the electrostatic pulses more rapidly than SO_4^{2-} ions. However, this of itself this does not infer that the energetic response is of a purely chemical and enthalpic nature.

7. Statistics Summary

To evaluate the statistical significance of the means against the charging method, a one tailed t-test was conducted. The results, with p-values of 3.91 x 10^{-16} for Pb-Acid and 7.69 x 10^{-10} for $LiFePO_4$, clearly show that the raised mean CoP values measured under IPC conditions are a direct consequence of the inductive pulse charging and not an artefact of the population distributions.

	Pb-Acid		$LiFePO_4$	
CoP	***Control***	***IPC***	***Control***	***IPC***
X	0.69	1.78	0.79	8.87
σ	0.03	0.21	0.03	0.98
ΔCoP				
X	± 0.15	± 0.21	± 0.17	3.36
σ	0.007	0.022	0.007	0.31
t-test	t = -22.91, p = 3.91E-16		t = -10.78, p = 7.69E-10	

Table 3: Statistics summary for both batteries

The overall uncertainty ranges, calculated from a combination of the uncertainties for each of the measurements stages and the discharge correction, increase with the larger CoP values derived, as shown by the error bars in the various plots. In the control tests, the variability of the results is less than with the IPC tests. In the former, the uncertainty ranges of all the values overlap each other, meaning that they are essential the same value across each of the populations. With the IPC measurements, the variation was considerably larger, substantially reducing the mean CoP value down from between 12 and 14 to 8.87. This appears to be mainly due an effect referred to as 'conditioning', whereby a battery's response improves with continued IPC and reaches a plateaux, but which reduces significantly with inactivity of at least 3 hours, and more noticeably overnight. This phenomenon is explored under '*Other Observations*'.

[9]Li^+ ions, intercalated into a $FePO_4$ cathode at the positive terminal, have a higher thermodynamic Gibbs energy than SO_4^{2-} ions in a Pb-Acid battery.

A summary of the statistics for the derived CoP values, their associated uncertainty ranges and the single tailed t-tests is shown in **Table 3.**

8. Closed-Loop Tests

Closed-loop tests involve using some of the extra energy available to supply the input energy requirements of the pulse generating device. **Figure 8** depicts the situation as a modification to an open system with the 'Reused Output'. While this so called closed-loop operation is theoretically sound, so long as the output has sufficiently low entropy, in the case where batteries are the main energy receiver and dissipator, there are several reason why this can only be achieved using battery swapping, in effect incorporating a short delay into the availability of the energy.

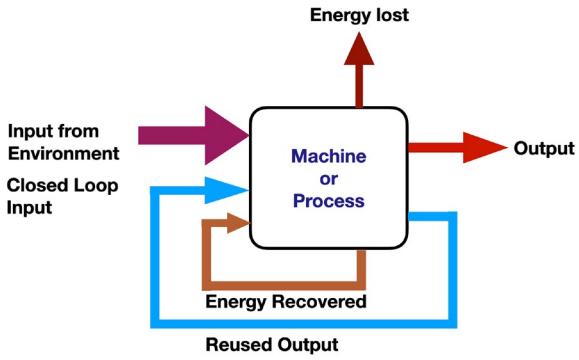

Figure 8: Energy reused in 'closed-loop' operation

Firstly, batteries cannot self-partition to allow such charging and discharging to happen simultaneously due to the internal chemical dynamics. Secondly, batteries need a certain amount of time to process incoming and outgoing energy flows and to convert electron exchanges into chemical changes and vice versa, as part of the reversible redox reactions taking place at the electrodes and in the electrolyte bulk [22]. In Lithium batteries, the intercalation processes at each electrode are heavily influenced by ageing phenomenon involving fractures and deformations of the electrode materials [23]. Such internal processes are why reading the true battery voltage is only done after a period of stabilization and recovery, as utilised in the CoP and control measurement methodologies.

In battery swapping there are therefore two batteries, one that at any moment is providing the energy to run the system while the other battery is being pulse charged. Then, at a suitable interval, the batteries roles are rapidly reversed by relays operated by a ripple binary counter run with an oscillator to allow a user set interval. Given that the charge battery will have received more energy during pulse charging than it used in supplying the system in its previous supply stage, then some of this excess energy can be used to power the circuit and, potentially, an additional external load. In so doing, after a series of swap cycles, the battery will remain at a voltage equal to or higher than at the start of the process.

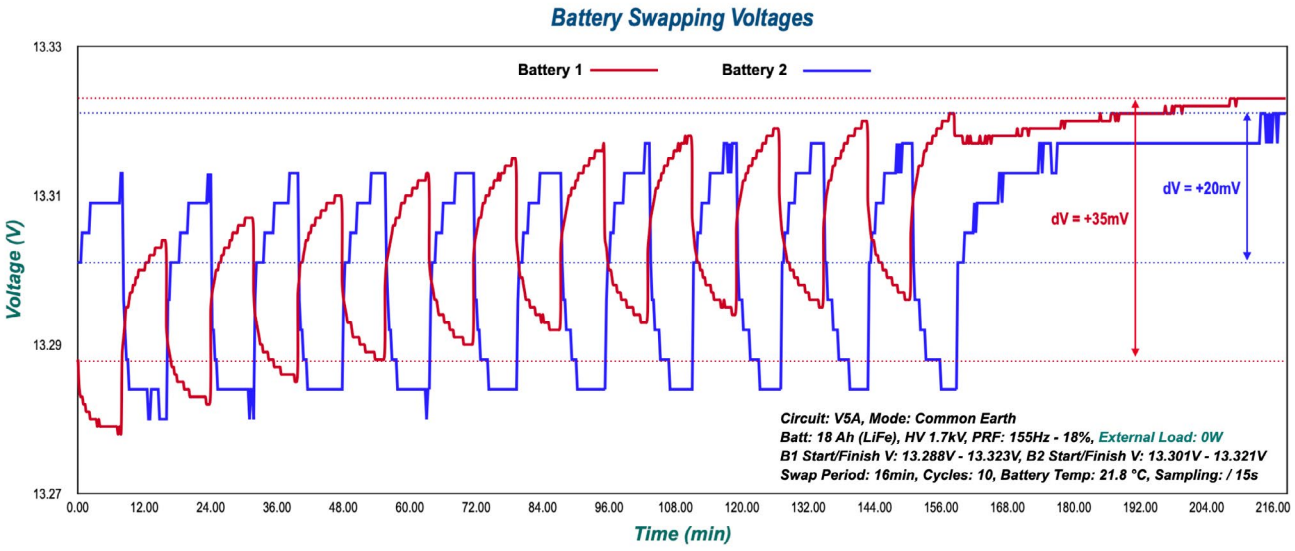

Figure 9: 'Closed-Loop' test with $LiFePO_4$ battery and with no external load

Figure 9 shows the monitoring of two $LiFePO_4$ batteries used to demonstrate a 'closed-loop' operation. Voltage sampling was undertaken every 15s by the CBA unit and a recording digital multimeter (RDM) and which was later exported and plotted.

In this first example, there was no additional external load and, over the duration of the approaching 4 hour test, including the 60 mins recovery, the voltages on both batteries gradually increased throughout. Here the 'energy influx' was able to run the device, offset the device's internal losses and also charge both batteries. In the context where a pulse motor is acting as the trigger to generate the pulses, an option available with the test rig used, then both batteries could maintain a state of constant or full charge while generating a small amount of useable mechanical energy from the rotor.

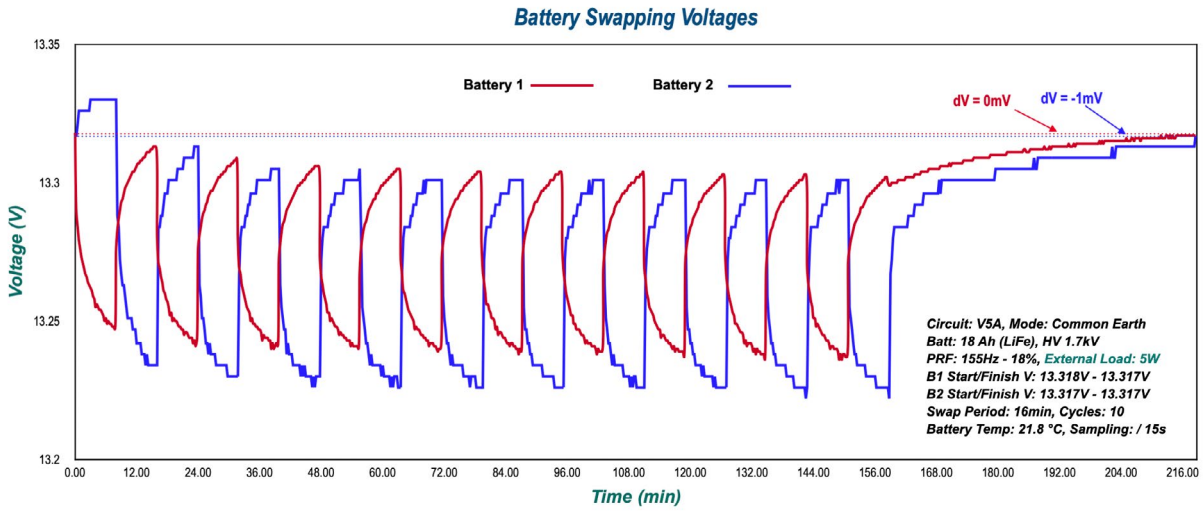

Figure 10: 'Closed-Loop' test with an additional 5W external load

In **Figure 10,** an additional external 5W load was added to the supply and the voltage drops as expected to start with but then remains stable and recovers after switch off to a figure at or near the starting voltage. A small reduction of the load would have maintained the voltages throughout the test and, in some preliminary work, a 5W load achieved that.

9. Other Observations

Alongside the CoP measurements and 'closed-loop' operation, various other observations were made regarding the apparent dynamics of the energy influx and the response of the batteries.

9.1. Charging Dynamics

One of the more surprising findings is the evidence to suggest that, what is being referred to as the 'energy influx', operates with a different dynamic to the regular battery charging process. The plot of a 'Vt' charging graph, such as monitored by the CBA unit, results from the well understood dynamics and thermodynamics of the electrolyte ions in the electrochemistry, as reflected in the Nernst equation that essentially correlates the Gibbs energy to the standard cell voltage E_0. However, the measurement data obtained paints a different picture of the observable charging, as shown on a graph, compared to the overall energy available via a subsequent discharge. With reference to **Figure 11,** the electrical energy being supplied to the pulse generator is a linear function of time, here shown by the blue line for the charging of a $LiFePO_4$, 18Ah battery. In contrast, the red line depicts a theoretical proposal of how the 'energy influx' appears to change with time. The optimum CoP measurement occurs when the 'energy influx' is greatest for the amount of energy supplied, in this instance at 8 minutes. Charging for longer will linearly increase the input energy but not increase the 'energy influx' by the same factor, which would be required to maintain the same derived CoP value.

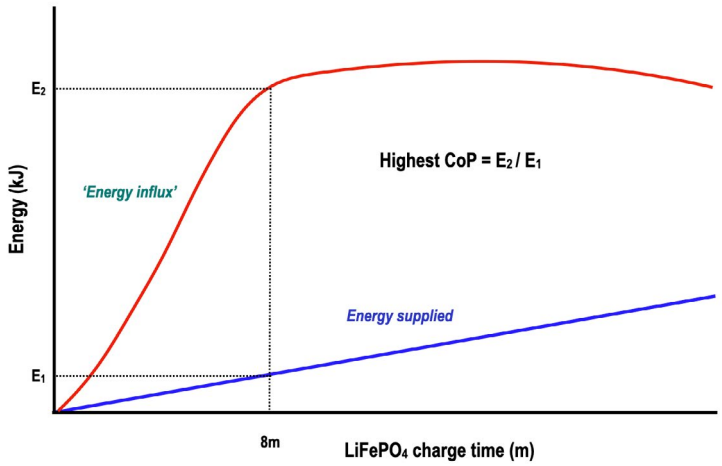

Figure 11: The apparent dynamics of the 'energy influx'

As such, longer charging times result in lower CoP values. Indeed extending charging times for several hours used in one session, so as to mimic the total charge (Ah) that might be delivered by regular mains charging, results in the CoP dropping below 1. In effect the red and blue lines eventually cross over as the input energy rises to meet the plateaued or dropping 'energy influx'. Similarly, with shorter charging times, the ratio is again lower and the optimum pulse charge time is a feature of a specific battery and charging parameters and can only be found by experiment. An alternative approach, to offset this diminishing effect, is to pulse charge for short times interspersed with rest intervals to allow the internal assimilation process to complete. While this method will still result in a CoP>1, unless the assimilation periods are carefully assessed and tailored for the specific battery and setup, the performance will still tend to be lower.

9.2. Estimation of 'Energy Influx'

Estimating a figure for the total influx can be of value in assessing the overall behaviour and dynamics of the system. In an open system the total useful energy output is a combination of the operator supplied input energy, moderated by the internal efficiency, added to any additional energy entering the system and which is also moderated by internal losses. Since the source and mechanisms of the additional energy input, the influx, is currently unknown, we cannot determine the effect or magnitude of any internal losses on this component. Using a previously determined value of the internal efficiency of 0.34, we can then determine the energy that would be required to bring the device up to a CoP of 1.0, in other words to completely offset the losses incurred by the low internal efficiency.

This is simply:

Input energy / η *Equ. 1*

Next we can calculate the energy required to take the output from a CoP = 1 to the actual measured CoP, e.g. 8.15. As stated, this ignores any losses incurred by the influx itself and is estimated in this example as:

Input energy x (8.15 - 1) *Equ. 2*

%Duty	Input Energy (kJ)	Efficiency η	CoP	Energy to CoP=1 (kJ)	CoP-1	Energy to CoP value (kJ)	Total 'Energy Influx' (kJ)	Total Power Influx (W)
26	1.51	0.34	8.15	4.44	7.15	10.80	15.24	31.7
28	1.77	0.34	6.96	5.21	5.96	10.55	15.76	32.8
30	2.03	0.34	5.09	5.97	4.09	8.30	14.27	29.7

Table 4: Influx estimates with varying % duty and user energy input

The summation of these two values gives us an estimate of the total energy influx from all sources and, dividing this value by the charge time, gives a value for the 'power influx'.

'Power influx' = Total energy influx / charge time *Equ. 3*

Table 4 lays out some values and where it can be seen that, for a range of %duty values, resulting in an increase in the supply current and consequent input energy, the total influx energy is fairly consistent to within ±5%, despite the derived CoP falling in line with the increased supply energy.

9.3. Effect of Mmf

From various preliminary test results, it has been observed that the energy influx is heavily influenced by the MMF[10] of the coils rather than by just the reverse flyback high voltage electrostatic pulses induced by the collapsing magnetic fields. This deduction is further supported by the effect of 'magnetic biasing' as shown in **Figure 14.** The presence of the rotor, with its inbuilt magnets, adds significantly to the magnetic flux in the coils and to the resulting CoP. Removing the rotor reduces the CoP by as much as 12% and yet, by replacing it with ceramic biasing magnets on the coil ends, the CoP is returned to its higher value. to the increased coil resistance. The is one of the main current limiting measures available,

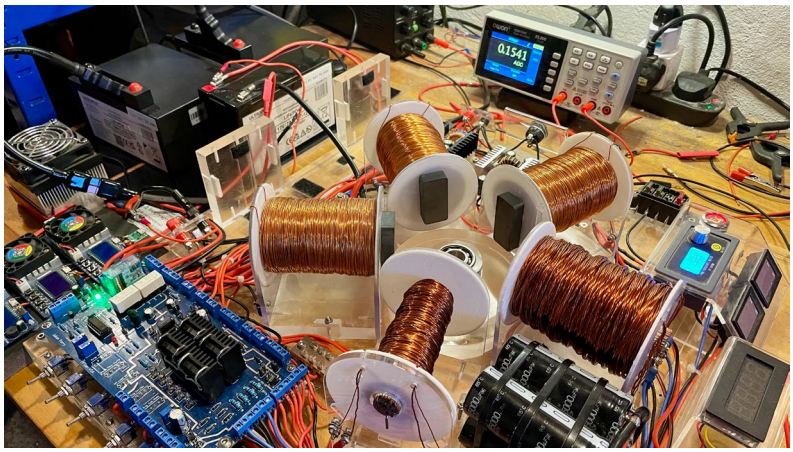

Figure 14: Magnetic biasing of the coils for use with a 7Ah $LiFePO_4$ battery

Within limits, raising the MMF of the coils serves to maintain the energy influx while at the same time lower the supply current due the other being to lower the % duty of the PWM trigger. Raising the MMF can be done by using a larger number of turns of thicker coil wire, resulting in the same overall resistance but a higher Ampere-Turns and magnetic flux. Alternatively, coils can be linked in series instead of parallel to raise the ohmic resistance while maintaining the AT and resultant MMF. **Figure 15** shows a set of measured values for a single coil, and where the AT value of 600 is the product of number of turns and the current of 0.24A. By joining three coils in series, the AT value has been raised to 825 while the supply current has been reduced to 0.11A. This both increases the MMF while reducing the user energy input from the solenoid supply current.

[10]*MMF is the Magneto-Motive-Force in a magnetic circuit, analogous to EMF in electrical circuits. The main factor for its value in a coil is the Ampere - Turns (AT).*

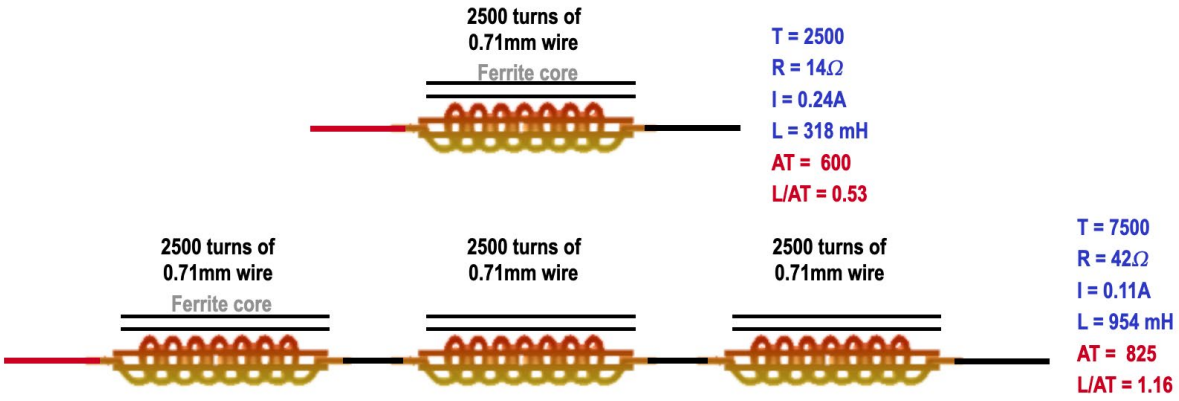

Figure 15: The effect of changing the number of coils and their configuration

The ratio of L(mH) to AT gives a useful ranking order for the CoP performance between the arrangements, but not a relative and numerical indicator of the CoP. A parallel arrangement would give the poorest result, then the single coil and the best with the three in series. While the highest ranking is with the 3 coils in series, the charging rate will be the lowest due to the minimal current. As has been noted, the energy influx presents as one of two components contributing to the overall energy state of the battery and the coil configuration needs to be experimented with for the best overall result. With some batteries a higher conventional charging rate may be useful and, for the study, a parallel arrangement was used with just 3 coils and found to give acceptable CoP results when used with the other settings, especially with $LiFePO_4$ batteries.

9.4. Battery Conditioning

Another important observation is one that lends some credence to the idea that a battery undergoing IPC experiences a process referred to as 'conditioning'. This proposes that a new battery, that has never undergone IPC will, over a number of cycles that depends upon the battery type, improve its performance with time. With Pb-Acid batteries this occurs over 10 - 20 IPC sessions (partial and not full capacity charge and discharge cycles). With the $LiFePO_4$ batteries, this occurs much faster, in the range of 5 - 8 sessions. Similarly, smaller changes in response to IPC can take place over shorter times, such as when a battery is inactive overnight or after a rest of 3 or more hours, although when using full charge/ discharge cycles the response can be maintained for several days.

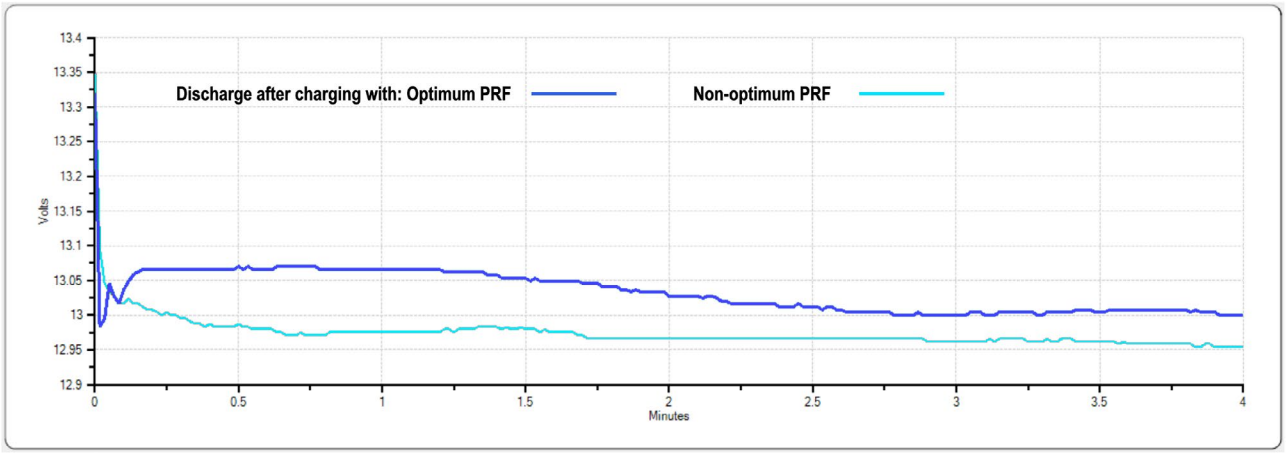

Figure 12: Discharging after IPC with optimal and non-optimal PRFs

The improvement in response can also be seen during discharges. **Figure 12** displays a pair of curves for identical discharges of a larger 40Ah $LiFePO_4$ battery. With the light blue trace the battery was previously pulse charged at a PRF

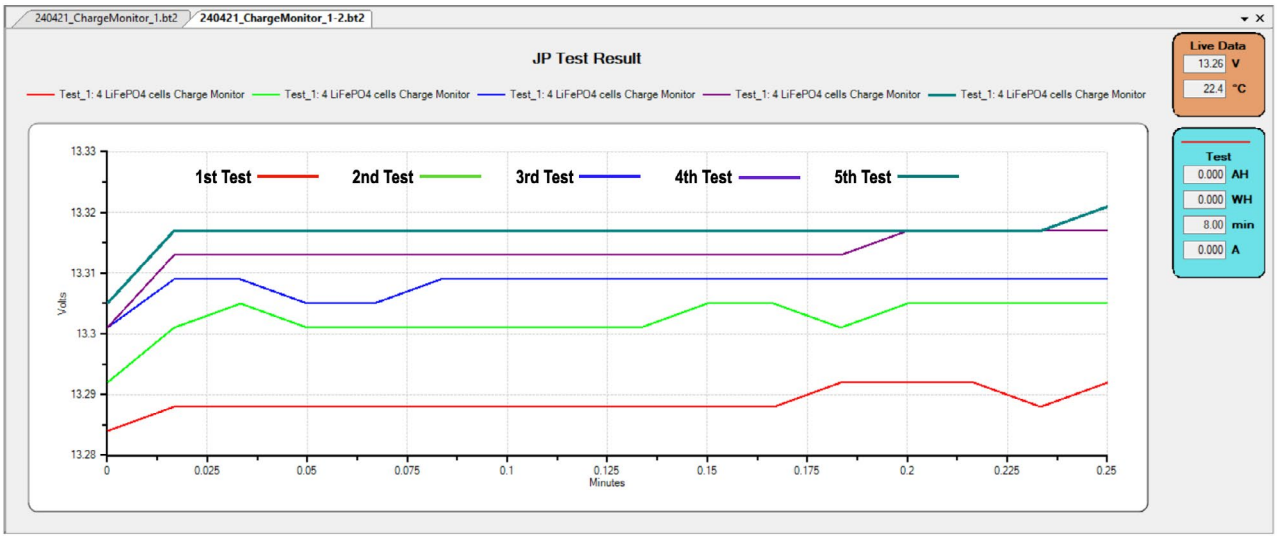

Figure 13: Sequential charging sessions showing improving response

of 140Hz, which was not its optimum value and, with the dark blue trace after IPC at the optimum PRF of 172Hz. In contrast to the typical shape of a discharge curve, after IPC at the optimised PRF, there is a rise in voltage soon after the initial drop, indicative of a charging process continuing on after pulsing has ceased, and to some extent off-setting the voltage and energy drop in the battery over the remainder of the 4 min discharge. This phenomenon is further evidenced in a sequence of IPC sessions carried out in succession. This is depicted in **Figure 13** where the start of five sequential charging sessions have been overlayed and where it indicates a faster response with each charging event. Again, since we do not yet know the full nature of the all charging processes, we are unable to correlate the observed changes in dV/dt with the resulting measured CoP values.

10. Discussion

The term CoP has traditionally been used with heat pumps that employ well understood energetic pathways in creating a suitable energy gradient for thermal energy to flow from the local environment into the device. Internal efficiency then moderates both the user input and the heat influx to produce a net output and where the total energy output is a multiple of the total user supplied energy input. Since CoP is simply a unitless ratio of energy values, it can be applied in any context where additional energy is being realised in the whole system, whatever its source.

While the main hypothesis of achieving a CoP>1 has been demonstrated, in the context of IPC a calculated CoP only applies to a specific set of operational parameters and is therefore not a useful characterising feature of the system as a whole; a common misconception. Instead, the power influx value may serve this role better since it appears more consistent over a range of parameters. These parameters include the coil configuration and load voltage, the pulse peak kV with its trigger PRF and duty cycle, as well as the placement of charging on the charging profile. The validity of the CoP values derived has also been supported by 'closed-loop' operation, even if only using a small external load, and shows that the energy influx is sufficient to offset the poor internal efficiency and also gradually charge both batteries.

Based on the behaviour of the influx over the duration of a charging event, it is reasonable to state that the observable battery charging, based on the reversible redox reactions and as represented on a 'Vt' charging profile, is not synonymous and identical with the energy influx, but rather that there is a relationship between the two processes, the exact nature of which has yet to be determined. A fast battery charging rate is generally associated with a low CoP value, and the converse generally applies.

The way in which the effect of the electrostatic pulses propagates throughout the battery, whether it is made of a few large area plates or many smaller capacity cells, as in a Lithium battery design, also suggests another process and dynamic at work. Further research into both IPC and more conventional (non-inductive) forms of pulse charging with Lithium batteries may yield further insights into ways to extend battery life and performance [24]. However, until such time as there is greater clarity regarding the energetic pathways involved, whether they originate from inside or outside of the battery, such conjectures cannot contribute to a working model.

The observation that a battery improves its performance over time if it has never been exposed to IPC, a process referred to as 'conditioning', is likely linked to the observed continuing charging effect after HV pulsing has ceased. This suggests an adaptation process taking place and where an ongoing effect in the electrolyte contributes to maintaining the energy state of the battery during discharge and in subsequent charging sessions. This 'after-effect' subsides with time to a significant degree depending on whether full or partial charge/discharge cycles have occurred.

The higher response of $LiFePO_4$ batteries compared the Pb-Acid may be linked to the higher Gibbs energy of the Li+ ions intercalated with the host matrix, or to their lighter mass. However, this does not necessarily mean that the origin of the excess energy is from the electrochemistry itself, since it is also

reasonable to propose that the less massive and more mobile Lithium ions are better able to respond to an energetic and 'far from equilibrium' event, and more easily translate that event into conventional electron flow and ion exchanges in the normal manner.

The evidence so far indicates that there are two aspects to the total charging process, one represented and observable as a 'Vt' graph, and another that is more difficult to identify but which is only partly reflected in the regular observable charging process. For the former, the graph is driven by the thermodynamics of the various reversible redox reactions taking place at the electrodes and in the electrochemistry, and which are governed by such quantities as the Gibbs energy related to the making and breaking of relevant chemical bonds and ionic exchanges [22]. The other process, associated with the energy influx, operates on a different time scale and output CoP measurements are sensitive to the operating parameters of PRF, coil configuration and MMF, coil voltage, charging time and internal resistance. The existence of longitudinal waves along the coil's main axis have also been observed by other researchers, and which was a particular focus for Nikola Tesla in his power transmission experiments [25], but this has not been explored in this study.

Unless all the operational parameters are finely tuned for a specific battery and setup, then the CoP can easily fall below one and into the range of the control values from regular charging. This may explain why other investigators have often found obtaining consistent results hard to achieve.Despite the clear role and effect of those factors that determine the rate of electrochemical and redox reactions, such as temperature, electrolyte ion concentration and pulse frequency, none of these provide a direct insight into whether the energy gains are arising from the electrochemistry itself rather than through it. At this time, the source of the additional energy input is therefore unclear but the options are evidently binary. Either it arises from within the electrochemistry itself, in direct response to the electrostatic pulses, or from the local environment by energetic pathways and processes not yet understood or recognised. Which of these options is the most likely is the subject of a follow-up study using battery 'State of Health' measurements [26,27] alongside quantitative chemistry and thermodynamic calculations with a 'chemical deficit' model. Here the possible loss of active chemical agents used to derive the energy influx would result in a reduction in charge capacity with continued use. Any correlation between energy influx and loss of charge capacity can therefore be established without monitoring a battery for the whole of its lifespan.

[11]*The rationale and method for measuring this is addressed in a pre-print by the author entitled 'Measuring Battery Health - Secondary Cell Dynamics and Electrochemistry' available at osf.io/7jhqt*

If the former option is the most likely, and chemical bond energy is being used as a form of 'fuel', then questions arise regarding the mechanisms of how voltage transients result in a preferential release of energy manifested as the transfer of charge amongst the electrodes and electrolyte ions, as opposed to the generation of low-grade enthalpic heat, of which none was observed. Should the latter option turn out to be the most likely, then that carries with it a need to reconsider some aspects of current quantum and classical electrodynamic theory. This will need to account for the availability and structuring of a form of otherwise ambient energy, from the vacuum or otherwise and presumably of an electromagnetic nature, and which, when a 'far from equilibrium' state is induced, results in a directed energy flow into a suitably receptive open system. Such systems, operating under the principles of dissipative and negentropic structures [28,29], are more appropriately described by the field of open thermodynamics in contrast to the conventional model. The larger electrodynamic and thermodynamic models integrate the local environment into their formulation rather than ignoring cross-boundary energy exchanges and being defined as a closed system with rigid boundary conditions [20].

11. Conclusions

The study has demonstrated that IPC can yield a CoP>1 with specific operational parameters compared to standard mains charging in two battery types and capacities. This has been further substantiated by 'closed-loop' tests and where the energy influx appears to posses a different dynamic to that of conventional charging. Evidence supports a continuing effect upon the electrochemistry after IPC has ceased. However, without a working model, the terms often used to describe this effect are of little descriptive value. Lithium Iron Phosphate batteries have shown themselves to be far more responsive to IPC and yield much higher CoP values. This may be due to their chemical makeup and the properties of Lithium ions. Nevertheless, they also exhibited higher variability in response, being more sensitive to the various operational parameters, inactivity and most likely to other stochastic processes within their electrochemistry.

A follow-on study will determine the most likely source of the energy gains and their implications for either the behaviour of battery electrochemistry in the context of high voltage transients, or for open thermodynamics in an electrochemical and electrodynamic context. This study will also establish the validity of various claims of benefits to battery SoH with their implications for battery management. Developing a valid theoretical model for IPC can only arise after further confirmation of the source and, until such time, it is unclear if IPC can serve as a useful low-powered energy source. In the meantime, various speculative theories have been proposed based on the extrapolation of current electrodynamic and quantum based theories. Here, there is good reason to believe that extended, non-linear and non-equilibrium operating and boundary conditions can reveal some significant limitations of mainstream understanding. The Open Science Framework makes publicly available all the study materials, together with detailed materials for replication, to enable others to gather further insights into this important phenomenon and experimental topic.

Replication

Replication information is provided in the form of a comprehensive *'Assembly & Guidance'* manual, PCB schematic and printing files and a range of other supplementary documents and materials at: osf.io/54qcn/

Acknowledgments

The support of Dr Glenn Ramsey is acknowledged in proof-reading the manuscript, various of the study methodologies and being a 'read' contributor to the project.

References

1. Kurzweil, P. (2010). Gaston Planté and his invention of the lead–acid battery—The genesis of the first practical rechargeable battery. *Journal of Power Sources, 195*(14), 4424-4434.
2. Cook, D. M. (1871). Improvements in Induction Coils. US Patent 119,825A. *US Patent and Trademark Office*.
3. Nikola, T. (1893). On light and other high frequency phenomena. *Franklin Institute, Philadelphia*.
4. Aspden, H & Adams, R. G. (1993). Electrical motor-generator, *UK Patent GB2282708A*.
5. Gray Sr, E. V. (1987). U.S. Patent No. 4,661,747. Washington, DC: *U.S. Patent and Trademark Office.*
6. Raymond, K. (1968). U.S. Patent No. 3,374,376. Washington, DC: *U.S. Patent and Trademark Office*.
7. Lindemann, P., & Murakami, A. (2013). *Bedini SG-The Complete Intermediate Handbook*. Washington: A & P Electronic Media Liberty Lake.
8. Hunt, B. J. (2012). Oliver Heaviside: A first-rate oddity. *Physics Today, 65*(11), 48-54.
9. Myers, N. M., Abah, O., & Deffner, S. (2022). Quantum thermodynamic devices: From theoretical proposals to experimental reality. *AVS quantum science, 4*(2).
10. Lundén, M. (2016). A Rare Genius, Mr Gabriel Kron. LinkedIn.
11. Kelly, P. (2011). *A Practical Guide to 'Free-Energy' Devices*.
12. Sriphan, U., Kerdchang, P., Prommas, R., & Bunnang, T. (2018). Coefficient of performance of battery running and charging by magnet generator Bedini. *Journal of Electrochemical Energy Conversion and Storage, 15*(4), 041002.
13. Inam, H., & Al-Turjman, F. (2021). Intelligent free energy usage through radiant energy space phenomenon: An IoT-powered prototype for modified Bedini generator. *Microprocessors and Microsystems,* 104319.
14. Chrysocheris, I., Chatzileontaris, A., Papakitsos, C., Papakitsos, E., & Laskaris, N. (2024). Pulse-Charging Techniques for Advanced Charging of Batteries. *Mediterranean Journal of Basic and Applied Sciences (MJBAS), 8*(1), 22-36.
15. Ali, A. H., & Ismail, A. N. C. (2017). Design and simulation of self-running magnetic motor. *Journal of Engineering Technology, 5,* 27-31.
16. Murad, P. A., Boardman, M. J., Brandenburg, J. E., & Mitzen, W. (2020). A Nonlinear Electromagnetic *Device and Potential Explanations. science, 6*(12).
17. Sengupta, D. L., & Sarkar, T. K. (2003). Maxwell, Hertz, the Maxwellians, and the early history of electromagnetic waves. *IEEE Antennas and Propagation Magazine, 45*(2), 13-19.
18. Eckardt, H. (2007). How do space energy devices work.
19. Overduin, J. (2008). Gravity Probe B: Testing Einstein's Universe. Stanford University.
20. Sheehan, D. P. (2022). Beyond the Thermodynamic Limit: Template for Second Law Violators. *Journal of Scientific Exploration, 36*(3).
21. Lee, J. W. (2022). Type-B energetic processes and their associated scientific implications. *Journal of Scientific Exploration, 36*(3).
22. Schmidt-Rohr, K. (2018). How batteries store and release energy: explaining basic electrochemistry. *Journal of chemical education, 95*(10), 1801-1810.
23. Pender, J. P., Jha, G., Youn, D. H., Ziegler, J. M., Andoni, I., Choi, E. J., ... & Mullins, C. B. (2020). Electrode degradation in lithium-ion batteries. *ACS nano, 14*(2), 1243-1295.
24. Amanor-Boadu, J. M., Guiseppi-Elie, A., & Sánchez-Sinencio, E. (2018). The impact of pulse charging parameters on the life cycle of lithium-ion polymer batteries. *Energies, 11*(8), 2162.
25. Dollard, E. (2014). Electromagnetic Induction and its Propagation.
26. Braun, J. A., Behmann, R., Schmider, D., & Bessler, W. G. (2022). State of charge and state of health diagnosis of batteries with voltage-controlled models. *Journal of Power Sources, 544*, 231828.
27. Suozzo, C. (2008). Lead-acid battery aging and state of health diagnosis (Master's thesis, The Ohio State University).
28. Prigogine, I. (1975). Dissipative structures, dynamics and entropy. *International Journal of Quantum Chemistry, 9*(S9), 443-456.
29. Lefever, R. (2018). The rehabilitation of irreversible processes and dissipative structures' 50th anniversary. *Philosophical Transactions of the Royal Society A: Mathematical, Physical and Engineering Sciences, 376*(2124), 20170365.